HOKKAIDO UNIVERSITY

Title	Anisotropic surroundings effects on photo absorption of partially embedded Au nanospheroids in silica glass substrate
Author(s)	Meng, Xuan; Shibayama, Tamaki; Yu, Ruixuan; Ishioka, Junya; Watanabe, Seiichi
Citation	AIP Advances, 5(2), 27112 https://doi.org/10.1063/1.4908010
Issue Date	2015-02
Doc URL	http://hdl.handle.net/2115/58554
Rights(URL)	http://creativecommons.org/licenses/by/3.0/
Type	article
File Information	1.4908010.pdf

Instructions for use

Anisotropic surroundings effects on photo absorption of partially embedded Au nanospheroids in silica glass substrate

Xuan Meng, Tamaki Shibayama, Ruixuan Yu, Junya Ishioka, and Seiichi Watanabe

Articles you may be interested in

Ion irradiation synthesis of Ag–Au bimetallic nanospheroids in SiO2 glass substrate with tunable surface plasmon resonance frequency
J. Appl. Phys. **114**, 054308 (2013); 10.1063/1.4817725

Growth of oriented Au nanostructures: Role of oxide at the interface
J. Appl. Phys. **111**, 064322 (2012); 10.1063/1.3698505

Anisotropic surface plasmon excitation in Au/silica nanowire
Appl. Phys. Lett. **96**, 263106 (2010); 10.1063/1.3456529

Pulsed infrared laser annealing of gold nanoparticles embedded in a silica matrix
J. Appl. Phys. **103**, 083545 (2008); 10.1063/1.2909965

Synthesis of Au nanotubes with SiO x nanowires as sacrificial templates
J. Vac. Sci. Technol. A **24**, 1336 (2006); 10.1116/1.2172942

Anisotropic surroundings effects on photo absorption of partially embedded Au nanospheroids in silica glass substrate

Xuan Meng,[1,a] Tamaki Shibayama,[1,b] Ruixuan Yu,[2] Junya Ishioka,[2] and Seiichi Watanabe[1]

[1]*Center for Advanced Research of Energy and Materials, Faculty of Engineering, Hokkaido University, Sapporo, Hokkaido 060–8628, Japan*
[2]*Graduate School of Engineering, Hokkaido University, Sapporo, Hokkaido 060–8628, Japan*

The influence of a directly adjacent or an anisotropic surrounding medium alters the plasmonic properties of a nanoparticle because it provides a mechanism for symmetry breaking of the scattering. Given the success of ion irradiation induced embedment of rigid metallic nanospheroids into amorphous substrate, it is possible to examine the effect of the silica glass substrate on the plasmonic properties of these embedded nanospheroids. In this work presented here, discrete dipole approximation (DDA) calculations for the Au nanospheroids' optical properties were performed based on 3–dimensional (3D) configuration extracted from planar SEM micrographs and cross–sectional TEM micrographs of the Au nanospheroids partially embedded in the silica glass, and the well–matched simulations with respect to the experimental measurements could demonstrate the dielectric constant at the near surface of silica glass decreased after Ar–ion irradiation. © *2015 Author(s). All article content, except where otherwise noted, is licensed under a Creative Commons Attribution 3.0 Unported License.* [http://dx.doi.org/10.1063/1.4908010]

I. INTRODUCTION

Nanostructured noble metals exhibit remarkable optical properties due to the excitation of localized surface plasmons (LSPs) by incident light, which has stimulated considerable applications in diverse fields such as surface enhanced Raman spectroscopy (SERS),[1–3] solar cell,[4–7] and biosensors.[8] The past decades have witnessed an explosion in the use of plasmonic metal nanoparticles for light localization and near–field enhancement applications in tip enhanced Raman spectroscopy (TERS) which is capable in ultimately detecting individual molecular binding events.[1,2] Although surface enhanced Raman scattering can be achieved by exploiting the electromagnetic resonance properties of noble metal nanoparticles, chemically and thermally stable SERS platforms with high and uniform enhancements remain the focus of recent research.[1,3] Experimental and theoretical results indicate the frequency and strength of the light localization strongly depend on the size and shape of the nanocrystals, and their local dielectric environment.[9–15] Analyses of these plasmonic nanoparticles often consider isolated metallic spheroids in homogeneous environments, but few nanoplasmonic systems can be described this way, especially for commonly used systems composed of non–spherical metallic nanoparticles located on a substrate.

The influence of a directly adjacent or an anisotropic surrounding dielectric medium alters the plasmonic properties of a nanoparticle.[12–15] Here the substrate matters because it provides a mechanism for symmetry breaking of the scattering and supports an image dipole, shifting, broadening, and splitting the local surface plasmon resonance (LSPR) as pointed out recently for spherical

---

[a]Present address: Tianshuinan Road 222, School of Nuclear Science and Technology, Lanzhou University, Lanzhou 730000, China
[b]Author to whom correspondence should be addressed. E–mail: shiba@qe.eng.hokudai.ac.jp

5, 027112-1

and cubical nanoparticles.[13–15] This effect has been of tremendous interest in the development of ultrasensitive SERS and TERS, where individual nanoparticles are stabilized onto a dielectric substrate.[2,3] Theoretical models capable of incorporating substrate effects and asymmetric particle geometries have been developed based on the numerical approximations including the finite difference time domain method (FDTD)[3,12] and the discrete dipole approximation (DDA).[9–11,13–15] Specifically, the pioneering works focused on the optical response of Ag nanospheres embedded in silica glass was studied by DDA method, and the authors concluded that the LSPR shifted linearly towards the longer wavelength (red–shift) with the surface area of the embedded parts.[9]

Quantum beam irradiation techniques exist for studying plasmonic Au nanoparticles partially embedded in the substrates including laser irradiation,[12,16] electron beam irradiation,[17] and ion beam irradiation.[18–21] Ion beam irradiation of ultra–thin Au films evaporated on dielectric substrates presents a simple and reproducible way to fabricate plasmonic nanostructures with strong adhesive to the dielectric substrate due to the ion irradiation burrowing of the rigid metallic nanostructures into amorphous substrate.[18,20–22] Given the success of the experimental approach, it is very important to examine the effect of the silica glass substrate on the plasmonic properties of these embedded nanoparticles. In this work presented here, DDA simulations for the Au nanospheroids' optical properties are performed based on 3D configuration extracted from planar SEM micrographs and cross–sectional TEM micrographs, and we show that the well–matched simulation with respect to the experimental observations is possible to elucidate the dielectric constant at the near surface of the silica glass decreased under Ar–ion irradiation.

II. EXPERIMENTAL PROCEDURE AND RESULTS

In this study, Au thin films were evaporated on mirror polished silica glass substrates with an O–H density of ∼ 800 ppm (SH-200, Shin–Etsu Quartz Co., Ltd. Japan) at room temperature by electrically heating the Au source (purity, 99.9%) in a 6.0×10^{-5} Torr vacuum. The thickness of the Au films was estimated to be approximately 5.0 nm by comparing the color with that of the standard sample, which had been previously calibrated. Thermal annealing of these samples were conducted *ex–situ* under high vacuum (4.5×10^{-5} Pa) at 873 K for 10 minutes. While the as–deposited silica glass shows a blue color, the optical micrograph of the annealed samples exhibits a red color (Fig. 1(a), upper section). In addition, a field–emission scanning electron microscope (SEM; JEOL JSM–7001FA, Japan) was used to examine the surface morphology. In the SEM micrographs, the bright spots represent the Au nanospheroids and the dark parts represent the exposed silica glass. It is therefore evident that the Au film transformed into a layer of homogenously distributed Au nanospheroids (SEM micrograph in Fig. 1(a), middle section), due to the thermal induced homogeneous nucleation and surface tension extraction.[23] Photoabsorbance were recorded over a wavelength range of 300–800 nm on a spectrophotometer (JASCO V–630, Japan) with a bandwidth of 1.5 nm (Fig. 2(a)). The enhanced absorption band appeared around 530 nm was induced by the resonance of the incident visible light with the combined oscillation of the free electrons aggregated at the surface of these Au nanospheroids sustained on the silica glass, named localized surface plasmon resonance (LSPR).[20,21] In addition, the nanospheroids' vertical dimension was verified by transmission electron microscope (TEM; JEOL JEM–2010F, Japan), and the cross–sectional TEM samples were prepared using a focused ion beam equipment (JEOL JEM–9320FIB, Japan). The planar SEM micrograph combined with the cross–sectional TEM micrograph shows the Au nanoparticles has a spheroid morphology standing on the silica glass (TEM micrograph in Fig. 1(a), bottom section). Specifically, the Au nanospheroid has a round shape in the planar SEM observation, and it has an oval shape with the longitudinal dimension (diameter) larger than the vertical dimension (height) in the cross–sectional TEM observation. Therefore, the nanoparticles were proposed to have spheroid morphology and a 3D model abstracted from the real structure of Au nanospheroids has been developed to describe a simplified configuration of Au nanospheroid under Ar–ion irradiation (Fig.3).

100 keV Ar–ion irradiation at ambient temperature with fluences of 9.5×10^{14} cm^{-2}, 1.9×10^{15} cm^{-2}, 3.0×10^{15} cm^{-2}, 4.5×10^{15} cm^{-2}, and 6.0×10^{15} cm^{-2} were performed to study the fluence dependence. The energies of the ions were chosen such that the range is wider than the
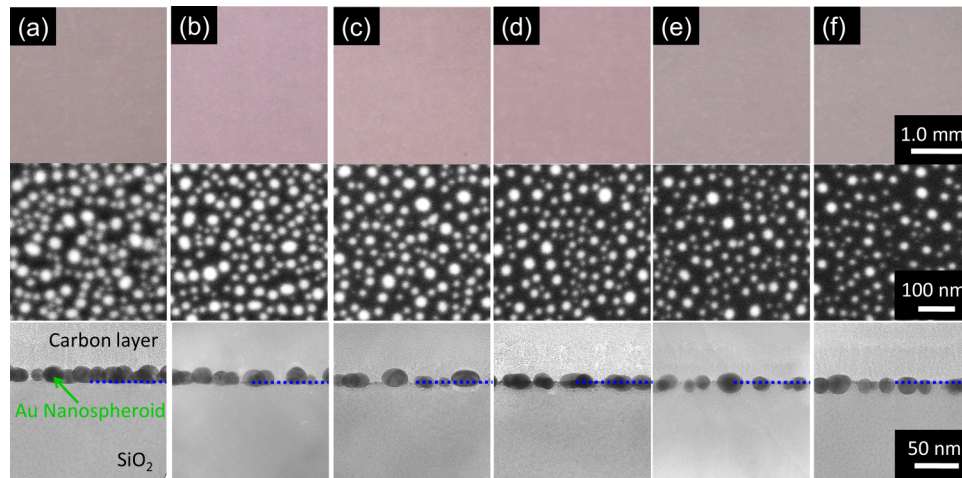
FIG. 1. Optical micrographs (upper sections of each panel), planar SEM micrographs (middle sections of each panel), and typical bright field cross–sectional TEM micrographs (lower sections of each panel) of (a) thermally annealed sample, and 100 keV Ar–ion irradiation of post–annealed samples to fluencies of (b) 9.5×10^{14} cm^{-2}, (c) 1.9×10^{15} cm^{-2},(d) 3.0×10^{15} cm^{-2}, (e) 4.5×10^{15} cm^{-2}, and (f) 6.0×10^{15} cm^{-2}.

vertical dimension (viz. height) of the Au nanospheroids, as calculated by the SRIM 2011 code,[24] leading to the deposition of the kinetic energy in the near surface of silica glass. Ar–ion irradiation on the samples was performed using the 400 keV ion accelerator at the High Voltage Electron Microscope Laboratory, Hokkaido University.[20,21] A low pressure of 10^{-3} Pa was maintained inside the irradiation chamber and Ar–ion beam was scanned with a current maintained at approximately $2.0\mu A\ cm^{-2} \cdot s^{-1}$. After irradiation, the enhanced absorption band was clearly observed for each specimen (Fig.2(a)), which is a characterization of LSPR with the band positions summarized in Table I. A significant shift of the LSPR band position towards the longer wavelength (red shift) was observed at the lowest irradiation fluence, and then gradually shifted towards the short wavelength from 540 nm to 530 nm with the further irradiation (Fig. 2(b)). In general, the intensity and position of the LSPR bands are closely related to the shape and surrounding environment of the Au nanospheroids, which will be discussed theoretically in the following.

The planar SEM and cross–sectional TEM observations were conducted to examine the 3D morphology for the Au nanospheroids after Ar–ion irradiation. Figures 1(b)–1(f) demonstrate the optical micrographs (upper sections of each panel), planar SEM micrographs (middle sections of each panel), and cross–sectional TEM micrographs (bottom sections of each panel) of Au nanospheroids after Ar–ion irradiation. An evolution of the Au nanospheroids' embedment into the silica glass substrate under ion irradiation was observed from the cross–sectional TEM micrographs. A detailed study of the Au nanospheroids was conducted by measuring the nanospheroids top–view aspect ratio, cross–sectional diameter and height, and the embedding depth of these Au nanospheroids (Table I). Figures 4(a)–4(b) illustrate the top–view aspect ratio, the cross–sectional diameter, the cross–sectional aspect ratio (the diameter divided by the height), and the embedding depth of the Au nanospheroids as a function of irradiation fluence. While the top–view aspect ratio kept a value approximately 1.1 with the Ar–ion irradiation, indicating the Au nanospheroids formed after thermal annealing remained to be round under Ar–ion irradiation, the cross–sectional aspect ratio shows a systematic decrease with the irradiation fluence and approaches a value of 1.0. It is therefore evident that the spheroidal Au nanospheroids becoming spherical under ion irradiation, which have been observed for the swift heavy ion induced reshape of Au nanoparticles in silica glass substrate.[25–27] In addition, the mean embedding depth increased with the irradiation fluence and the Au nanospheroids nearly thoroughly embedded into the silica glass when the irradiation fluence reached 6.0×10^{15} cm^{-2}. It has been concluded that these Au nanospheroids were embedded by ion irradiation enhanced viscous flow, considering the sputtering effects.[18]
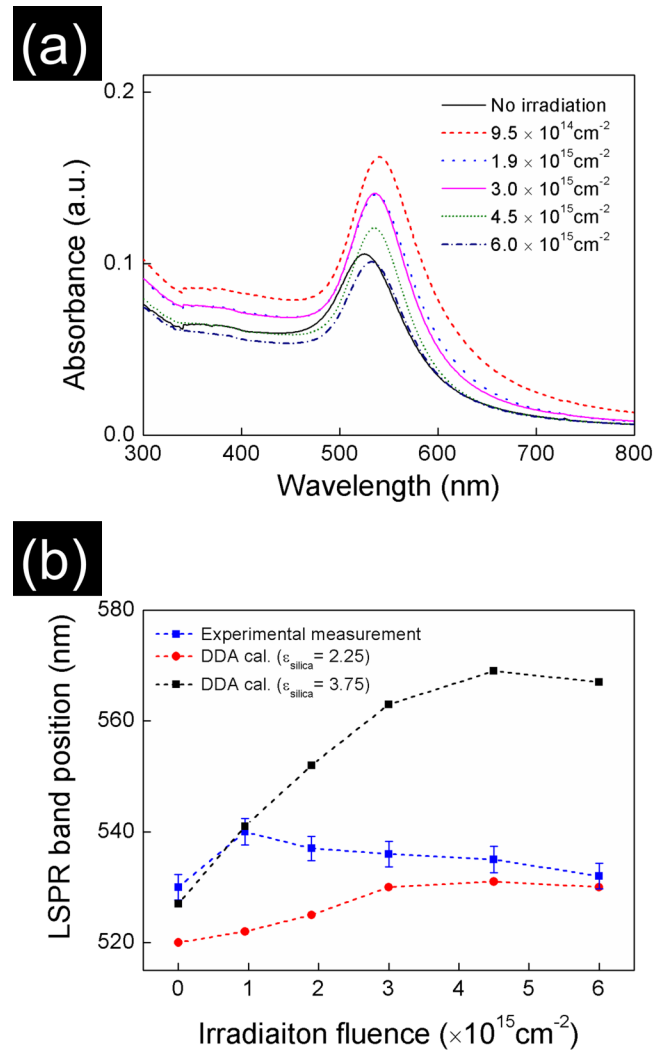
FIG. 2. (a) Photoabsorbance of the samples after 100 keV Ar–ion irradiation; (b) Experimentally measured and theoretically calculated LSPR band positions plotted as a function of irradiation fluence: the calculated LSPR band position with the silica glass dielectric constants 3.75 and 2.25 were shown in black solid square and red dot, respectively, and the experimental measured LSPR band positions were also given in blue solid square.

III. DDA CALCULATION OF PHOTO ABSORPTION COEFFICIENT

To interpret the enhanced photo absorption band shift resulting from the burrowing of Au nanospheroids into the silica glass substrate, the DDA method was applied to calculate the photo absorption coefficients of these Au nanospheroids partially embedded in silica glass. In this study, the software package DDSCAT7.3 developed by Draine and Flatau[28,29] was used. Because the size of the substrate is significantly larger than the nanospheroids, changing the substrate dimensions and geometries have non–negligible effects on the calculated optical properties,[10,11,13] substrate dimensions, geometries, and total number of dipoles were optimized in order to guarantee convergence in a reasonable amount of time without sacrificing accuracy. In these calculations, spheroid model was used to approximate the Au nanospheroid and the substrate was choosing to be a hemisphere with a diameter of three times larger than the Au nanospheroid (Fig. 3). It is noticed that the dielectric constant of the silica glass has a guaranteed value between 3.7 and 3.8; 3.75 was therefore chosen as the dielectric constant of the silica glass in the calculations. In addition, the wavelength–dependent dielectric function of bulk Au extracted from Johnson and Christy[30] was used. The accuracy has been confirmed by comparisons with analytical methods, in which Mie
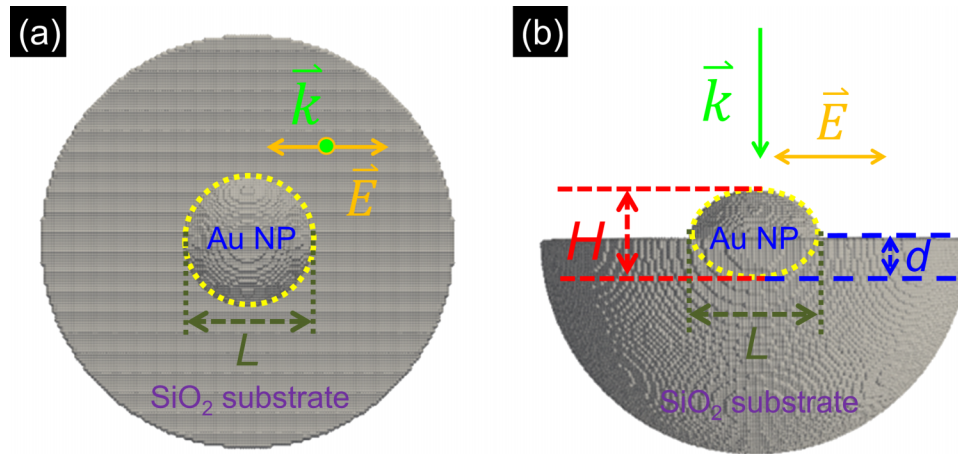
FIG. 3. A schematic illustration of the 3D model abstracted from the real structure of nanospheroids from planar SEM and cross–sectional TEM observation: (a) top–view and (b) cross–sectional configuration of the Au nanospheroid embedded in the hemisphere silica glass with lateral and vertical dimensions three times larger than that of the Au nanospheroid.

calculations of light scattering by a Au sphere was used.[31] Let us now use the DDA analysis to explore how the optical property responses to the geometrical parameters and the embedding depth and therefore the irradiation fluence of these Au nanospheroids.

Absorption coefficients of the nanospheroids were calculated by taking the external light incident normal to the top surface of the Au nanospheroid (Fig. 3(b)). In addition, Au nanospheroids' geometrical parameters obtained from planar SEM and cross–sectional TEM observation were used in the calculation. Finally, absorption coefficients with wavelengths from 300 nm to 800 nm were obtained and the wavelength spacing in the calculation amounts to 10 nm, where the band positions correspond to the LSPR wavelengths (Fig. 4(c)). Particularly, the substrate effect of silica glass on Au nanospheroids' optical responses was further investigated by near–field plasmon calculation. The plasmon field distributions were performed at the LSPR wavelength and the field distribution contours were obtained. Figures 5(a)–5(b) illustrated the field distribution contours for the Au oblate spheroid 20% embedded in the substrate, corresponding to the Au nanospheroid irradiated at a fluence of 9.5×10^{14} cm^{-2}. Here, the color axes show the E–field enhancement $\gamma = |E|^2/|E_0|^2$, where $|E_0|$ is the magnitude of the incident field and $|E|$ is the magnitude of local electric field surrounding the Au nanospheroid. Dipole like plasmon field distribution was demonstrated and the

TABLE I. Statistical results of Au nanospheroids geometrical parameters and optical properties of Au nanospheroids after Ar–ion irradiation.

Fluence ($\times 10^{15}$cm^{-2})	AR^{SEM} (nm)	L^{TEM} (nm)	H^{TEM} (nm)	d^{TEM} (nm)	LSPR^{DDA1} (nm)	LSPR^{DDA2} (nm)	LSPR^{Exp} (nm)
0.0	1.10 ± 0.10	23.8 ± 5.3	18.9 ± 3.8	2.0 ± 1.0	520	527	530.0 ± 2.3
0.95	1.08 ± 0.08	22.7 ± 6.0	16.9 ± 3.4	3.0 ± 1.0	522	541	540.0 ± 2.4
1.9	1.09 ± 0.09	21.9 ± 6.2	16.7 ± 3.5	5.0 ± 1.0	525	552	537.0 ± 2.4
3.0	1.10 ± 0.15	22.2 ± 4.7	16.8 ± 3.1	8.3 ± 1.6	530	563	536.0 ± 2.4
4.5	1.11 ± 0.16	19.2 ± 4.9	15.8 ± 3.3	10.7 ± 2.7	531	569	535.0 ± 2.4
6.0	1.09 ± 0.13	17.2 ± 3.8	16.5 ± 3.7	14.5 ± 2.7	530	567	531.0 ± 2.3

AR^{SEM} is the mean aspect ratio of Au nanospheroids obtained from planar SEM micrographs; L^{TEM}, H^{TEM}, and d^{TEM} are the mean longitude dimension (diameter), the mean vertical dimension (height) and the mean height embedded in the silica glass, obtained from cross–sectional TEM micrographs; LSPR^{DDA1} are the LSPR band positions of Au nanospheroids based on DDA calculation with the silica glass dielectric constant of 2.25; LSPR^{DDA2} are the LSPR band positions of Au nanospheroids based on DDA calculation with the silica glass dielectric constant of 3.75; LSPR^{Exp} are the LSPR band positions of Au nanospheroids measured from the experiment.
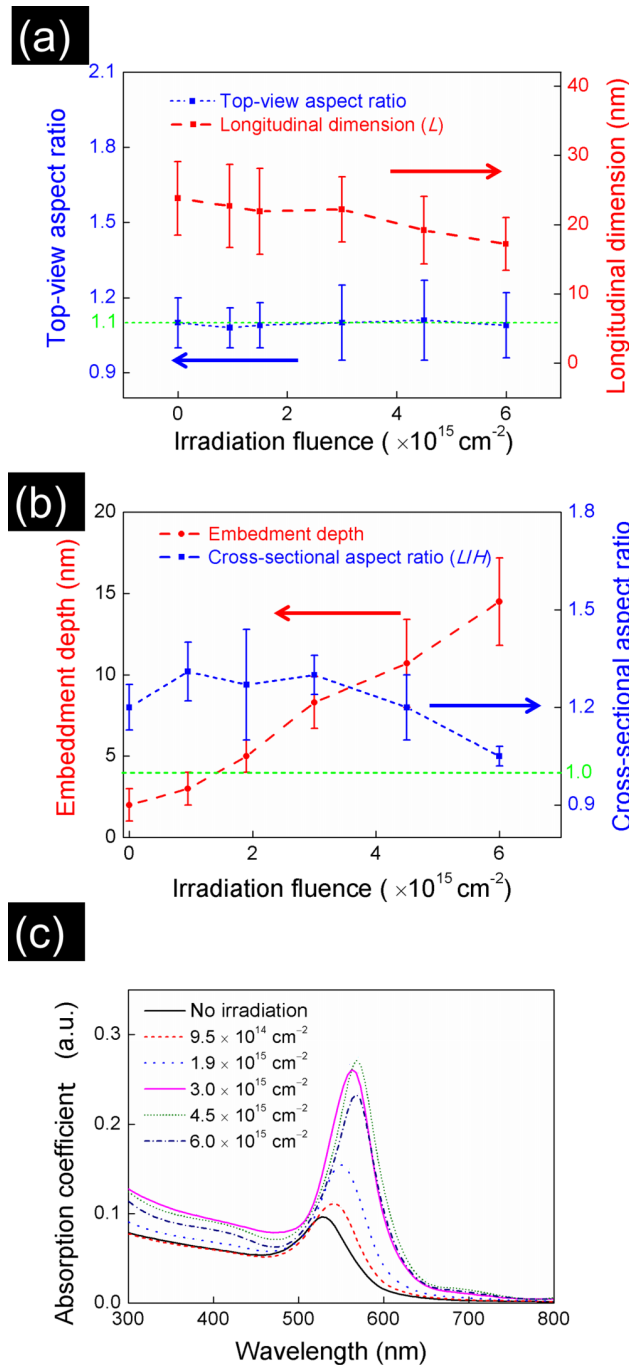
FIG. 4. Top–view aspect ratio (blue solid square) of the Au nanospheroids obtained from the planar SEM observation, and the cross–sectional diameter (red dot) of the Au nanospheroids obtained from the cross–sectional TEM observation, plotted as a function of irradiation fluence; (b) cross–sectional aspect ratio (blue solid square) and the embedding depth (red dot) of the Au nanospheroids obtained from the TEM observation, plotted as a function of irradiation fluence; (c) DDA calculated absorption coefficient plotted as a function of wavelength for the Au nanospheroids with the parameters obtained from the 3D models.

maximum enhancements occur at the junction regions between the Au nanospheroid and the substrate. Plasmon field distributions for the other oblate Au spheroids with different embedding depth were calculated at their LSPR wavelength, and it is noticed that they all have similar plasmon field distribution. It is evidence that the plasmon field is largely enhanced in the silica glass and this could
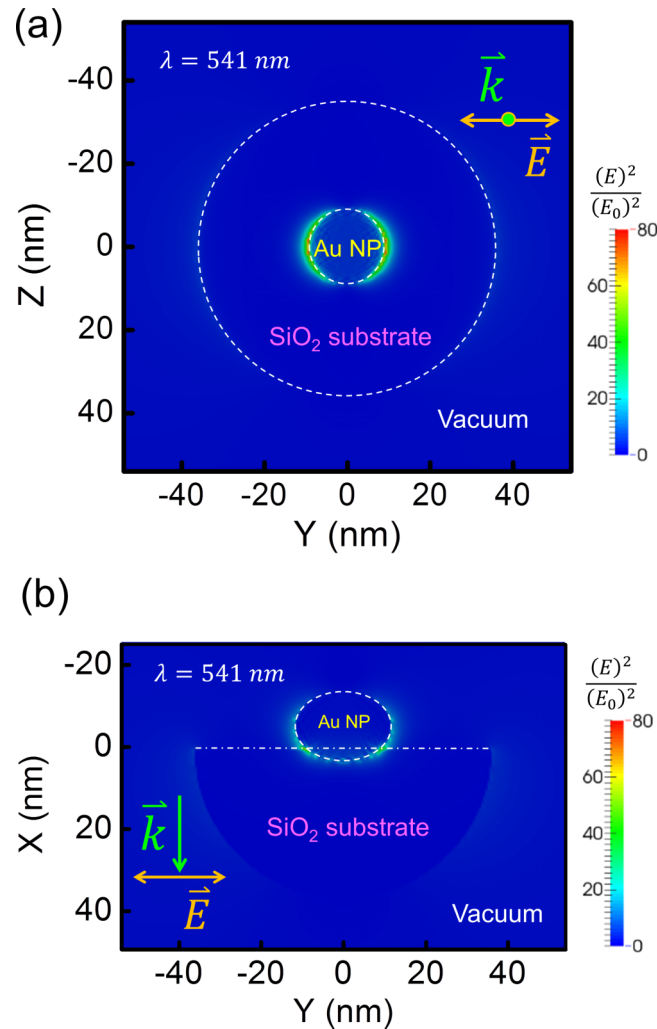
FIG. 5. The plasmon field distribution contours at the LSPR peak position (541 nm for Ar–ion irradiation fluence of 9.5×10^{14} cm^{-2}). In the DDA calculation, the light propagates along x–direction and is polarized along the y–direction, and the color axes show the plasmon field enhancement.

be understood to be a result of expected change of the gold electronic properties due to the increase of the oscillating electrons as a result of the interaction with the substrate.[10,12] Regions of strong local electric field enhancements were called "hot spots", which allows for maximum plasmonic coupling.[1–3] Since the Raman intensity depends on the electric field to the fourth power (E^4), each of the "hot spot" regions is able to produce a SERS enhancement factors exceeding 1000 if the molecule(s) of interest were located precisely in the 1–2 nm hot spot region.

Specifically, the dependence of the calculated LSPR band position on irradiation fluence and therefore the embedding depth is illustrated in black solid square in Fig. 2(b). It is noticed from DDA calculation that a red–shift of LSPR band position with the irradiation fluence was obtained. The trend of band shift with the characteristic embedding depth is well consistent with the experimental observations at the beginning of the Ar–ion irradiation ($<9.5 \times 10^{14}$ cm^{-2}). However, a discrepancy between the experimental and the calculated LSPR absorption band increases with the irradiation fluence and finally a large discrepancy of 40 nm was obtained at the highest irradiation fluence (6.0×10^{15} cm^{-2}). To interpret this large discrepancy, a decrease of the dielectric constant at the near surface of the silica glass (Fig. 6) was proposed to interpret this abnormal shift towards the shorter wavelength. Taking the decreased dielectric constant of the silica glass substrate into consideration, the dependence of the LSPR band positions on irradiation fluences
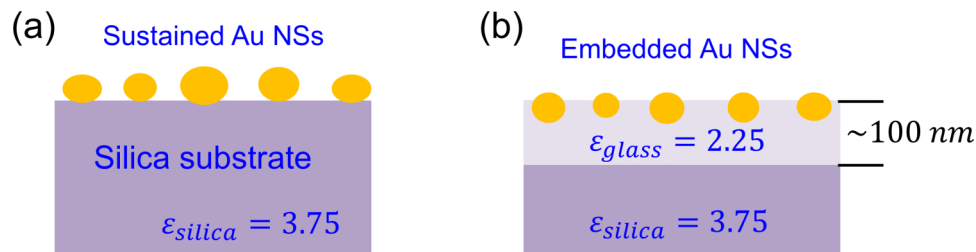
FIG. 6. A schematic illustration of the dielectric constant at the near surface of silica glass before (a) and after (b) 100 keV Ar–ion irradiation.

was recalculated (red dots in Fig. 2(b)), in which the dielectric constant of the silica glass substrate was chosen 2.25 corresponding to the general glass. It is noticed that the calculated LSPR band positions are well consistent with the experimental measurements at larger irradiation fluences (4.5×10^{15} cm^{-2} and 6.0×10^{15} cm^{-2}), while lower estimations were obtained at lower irradiation fluences ($<3.0 \times 10^{15}$ cm^{-2}). In addition, the experimental LSPR absorption bands in the medium irradiation fluences (from 1.9×10^{15} cm^{-2} to 3.0×10^{15} cm^{-2}) positioned in between of these DDA calculations based on the two substrates with dielectric constants of 2.25 and 3.75.

Also, a shift of the absorption band can be also driven by strong coupling between closely–spaced Au nanoparticles.[32,33] In order to take the coupling effect of closely–spaced Au nanospheroids (Au NPs) into consideration, a detailed study of the Au nanospheroids was conducted by measuring the nanospheroids gap width. The gap width of the Au nanospheroids as a function of irradiation fluence was given in Fig. S1 (see supplementary information[34]). It is noticed that the gap width increased with the irradiation fluence with the minimum value obtained at the irradiation fluence of 9.5×10^{14} cm^{-2}. To estimate the coupling effects between the closely–spaced Au NPs, the dependence of the calculated extinction coefficients on the gap widths were plotted as a function of wavelength (Fig. S2(b)). A shift of LSPR peak position towards the longer wavelength was observed with the decrease of the gap width was illustrated. It is noticed that the enhanced absorption peak obtained from the close–spaced Au NPs approaches that of the single Au NP's absorption peak when the gap width larger than 8.0 nm. In addition, all of the gap widths were larger than 8.0 nm from the SEM observation. Therefore, it is concluded that the coupling effects was weak and could be neglected.[34] It is therefore proposed that original silica glass at the near surface with a dielectric constant of 3.75 transformed into other forms of silica glass with a smaller dielectric constant (2.25) after Ar–ion irradiation, and a systematic decrease of the substrate's dielectric constant at the near surface with irradiation fluence was proposed.

IV. CONCLUSIONS

In summary, 100 keV Ar–ion irradiation of Au nanospheroids on silica glasses were performed to study the effect of the silica glass substrate on the plasmonic properties of partially embedded Au nanospheroids. It is evident that Au nanospheroids gradually became spherical and almost thoroughly embedded into the silica glass when the irradiation fluence reached 6.0×10^{15} cm^{-2}. Far–field and near–field discrete dipole approximation calculations were performed based on the 3D configurations extracted from planar SEM micrographs and cross–sectional TEM micrographs of the Au nanospheroids partially embedded in the silica glass. The well–matched calculations with respect to the experimental measurements could demonstrate the dielectric constant at the near surface of silica glass decreased from 3.75 to 2.25 after Ar–ion irradiation.

ACKNOWLEDGMENTS

[1] J. F. Li, Y. F. Huang, Y. Ding, Z. L. Yang, S. B. Li, X. S. Zhou, F. R. Fan, W. Zhang, Z. Y. Zhou, and D. Y. Wu, nature **464**(7287), 392 (2010).

[2] I. I. Naumov, Z. Li, and A. M. Bratkovsky, Applied Physics Letters **96**(3), 033105 (2010).

[3] P. Pavaskar, I.-K. Hsu, J. Theiss, W. Hsuan Hung, and S. B. Cronin, Journal of Applied Physics **113**(3), 034302 (2013).

[4] J. Yu, W. Shao, Y. Zhou, H. Wang, X. Liu, and X. Xu, Applied Physics Letters **103**(20), 203904 (2013).

[5] H. A. Atwater and A. Polman, Nat Mater **9**(3), 205 (2010).

[6] S. A. Maier and H. A. Atwater, Journal of Applied Physics **98**(1), 011101 (2005).

[7] K. Aydin, I. M. Pryce, and H. A. Atwater, Optics express **18**(13), 13407 (2010).

[8] A. G. Brolo, Nat Photon **6**(11), 709 (2012).

[9] K. L. Kelly, E. Coronado, L. L. Zhao, and G. C. Schatz, The Journal of Physical Chemistry B **107**(3), 668 (2002).

[10] Z.-Y. Zhang and Y.-P. Zhao, Applied Physics Letters **89**(2), 023110 (2006).

[11] C. Ungureanu, R. G. Rayavarapu, S. Manohar, and T. G. van Leeuwen, Journal of Applied Physics **105**(10), 102032 (2009).

[12] C.-Y. Chen, J.-Y. Wang, F.-J. Tsai, Y.-C. Lu, Y.-W. Kiang, and C. Yang, Optics express **17**(16), 14186 (2009).

[13] M. W. Knight, Y. Wu, J. B. Lassiter, P. Nordlander, and N. J. Halas, Nano letters **9**(5), 2188 (2009).

[14] P. Albella, B. Garcia-Cueto, F. González, F. Moreno, P. C. Wu, T.-H. Kim, A. Brown, Y. Yang, H. O. Everitt, and G. Videen, Nano letters **11**(9), 3531 (2011).

[15] S. Zhang, K. Bao, N. J. Halas, H. Xu, and P. Nordlander, Nano letters **11**(4), 1657 (2011).

[16] Y. Yoshida, S. Watanabe, Y. Nishijima, K. Ueno, H. Misawa, and T. Kato, Nanotechnology **22**(37), 375607 (2011).

[17] J. Biskupek, U. Kaiser, and F. Falk, Journal of Electron Microscopy **57**(3), 83 (2008).

[18] A. Klimmer, P. Ziemann, J. Biskupek, U. Kaiser, and M. Flesch, Physical Review B **79**(15), 155427 (2009).

[19] P. Gangopadhyay, S. K. Srivastava, P. Magudapathy, T. Sairam, K. Nair, and B. Panigrahi, Vacuum **84**(12), 1411 (2010).

[20] X. Meng, T. Shibayama, R. Yu, S. Takayanagi, and S. Watanabe, Journal of Materials Science **48**(2), 920 (2013).

[21] X. Meng, T. Shibayama, R. Yu, S. Takayanagi, and S. Watanabe, Journal of Applied Physics **114**(5), 054308 (2013).

[22] M. Ghaly and R. Averback, Physical review letters **72**(3), 364 (1994).

[23] C. V. Thompson, Annual Review of Materials Research **42**, 399 (2012).

[24] J. F. Ziegler, J. P. Biersack, and M. D. Ziegler, *SRIM, the stopping and range of ions in matter* (Lulu. com, 2008).

[25] Y. Mishra, F. Singh, D. Avasthi, J. Pivin, D. Malinovska, and E. Pippel, Applied Physics Letters **91**(6), 063103 (2007).

[26] K. Awazu, X. Wang, M. Fujimaki, J. Tominaga, H. Aiba, Y. Ohki, and T. Komatsubara, Physical Review B **78**(5), 054102 (2008).

[27] H. Amekura, N. Okubo, N. Ishikawa, D. Tsuya, K. Mitsuishi, Y. Nakayama, U. Singh, S. Khan, S. Mohapatra, and D. Avasthi, Applied Physics Letters **103**(20), 203106 (2013).

[28] B. Draine and P. Flatau, User guide for the discrete dipole approximation code DDSCAT7.3, http://arxiv.org/abs/0809.0337 (2013).

[29] P. Flatau and B. Draine, Optics express **20**(2), 1247 (2012).

[30] P. B. Johnson and R. W. Christy, Physical Review B **6**(12), 4370 (1972).

[31] P. Laven, Applied optics **42**(3), 436 (2003).

[32] P. K. Jain and M. A. El–Sayed, Chemical Physics Letters **487**, 153 (2010).

[33] J. Theiss, M. Aykol, P. Pavaskar, and S. B. Cronin, Nano Research **7**(9), 1344 (2014).

[34] See supplementary material at http://dx.doi.org/10.1063/1.4908010 for coupling effects of closely–spaced Au nano-spheroids.